

**M31 and Beyond:
Invited Reviews and Contributed Papers**

CFHT Wide-Field Deep Imaging of M33

J.-C. Cuillandre

*Canada-France-Hawaii Telescope Corporation, PO Box 1597, Kamuela,
HI 96743, USA*

J. Lequeux

Observatoire de Paris, 61 Av. de l'Observatoire, 75014 Paris, France

L. Loinard

*IRAM, 300 Rue de la Piscine, Domaine Universitaire, 38406 St Martin
d'Hères Cedex, France*

Abstract.

28' × 28' deep *V*- and *I*-band images of the center and of the SE field of M33 have been obtained at the prime focus of the Canada-France-Hawaii 3.6m telescope. They allowed to map separately the young blue stars, the red supergiants, the red giants and the extreme AGB stars. The disk as traced by red giants has a surprisingly sharp edge. The young blue stars trace the spiral structure very well, but the detailed comparison with H I and CO maps does not show a very good correspondence. The simple spiral-shock model of star formation proposed for the South arm of M33 is not confirmed. On the edge of the galaxy, star formation starts at a column density of H I of about 3×10^{20} atom cm⁻². The colour-magnitude diagram for the halo stars shows a broadened red giant branch with a mean metallicity [Fe/H] $\simeq -1.0$. The shape of the red giant branch confirms the distance modulus of 24.82 ± 0.20 for M33.

1. Introduction

M31 and M33 are the closest spiral galaxies. They are so extended that wide-field CCD mosaics are required to make deep studies of their stellar population over large regions. We have thus decided to observe a field in the outermost disk of M31 as well as in the disk and in an edge field of M33 using the 28' × 28' CCD mosaic at the prime focus of the CFH telescope, in the *V* and *I* (Cousins) bands. The purposes of these observations are to map extinction in the disks using the statistical reddening of the background galaxies, and to study the stellar populations. Preliminary results for M31 have been presented by Lequeux & Guélin (1996), but the data are presently being reduced anew. We present here preliminary results for the stellar populations of M33. The results for the extinction in the disk of this galaxy are not yet available. Section 2 presents the observations and their reductions. Section 3 discusses the distribution of the

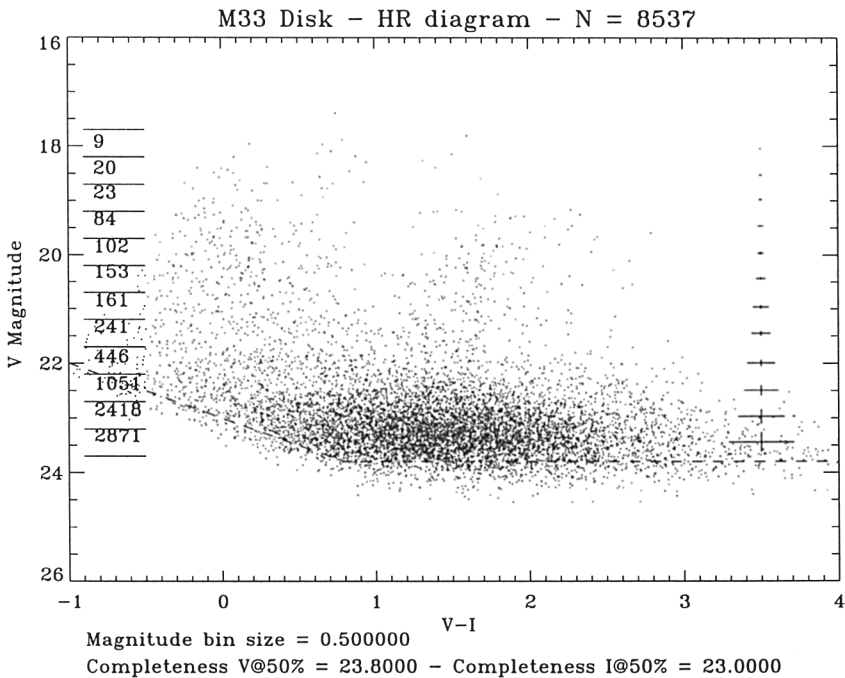


Figure 1. The V , $V - I$ color-magnitude diagram for stars in a field near the center of M33. The dashed line is the estimated 50% completeness limit. Estimated $1\text{-}\sigma$ errors on $V - I$ are indicated on the right.

various stellar population components. Section 4 compares the distribution of young stars with that of the gas. Section 5 discusses briefly the stellar population of the halo of M33.

2. Observations and Reductions

The observations have been made with the UH8k CCD camera at the prime focus of the CFH telescope. The UH8k mosaic is made of eight 2048×4096 pixel thick CCDs arranged to form a square. The scale is $0.206''$ per pixel and the field is $28' \times 28'$. The CCD at the upper right of the camera suffers from poor charge transfer efficiency and has not been used. The observations were made over two nights in October 1997 under non-photometric conditions with a seeing of $0.9''$. 3×5 min exposures were obtained in each of the V and I filters with the mosaic centered on the nucleus of M33, and 9×24 min exposures in each filter on the SE part of the galaxy. The relative response of the CCDs was obtained by observing large field photometric standards (Landolt 1992) and the zero points of the photometry were calibrated on isolated stars with published V and I photometry (Mould & Kristian 1986). We estimate the internal error (from CCD to CCD) to be 0.02 mag in each filter and the external error to be 0.05 mag in each filter.

The photometric extraction of the objects and the separation between stars and galaxies was performed using the recent version 2.0 of SExtractor (Bertin & Arnouts 1996). Details will be given elsewhere (Cuillandre et al. 1999). Approximate completeness limits for stars are $V=23$, $I=22$ for the central field and $V=25$, $I=24$ for the SE field.

Figure 1 shows the V , $V - I$ color-magnitude diagram for the stars in a disk field near the center of M33. One distinguishes clearly the blue stars of the main sequence around $V - I \simeq 0$, the bright red supergiants around $V - I \simeq 1.5$ (with some contamination by Galactic red dwarfs), the numerous brightest red giants with $V \leq 22.5$ with the extreme AGB stars at $V - I \geq 2.5$. Selecting parts of the V , $V - I$ diagram allow to map the respective populations over the face of the galaxy. Table 1 indicates the selection criteria we have used.

Table 1. Selection criteria for stellar populations.

Population	Mag. limits	Color limits
Blue stars (center)	$16 < V < 21.5$	$-1.0 < V - I < 1.0$
Blue stars (SE)	$16 < V < 23.5$	$-1.0 < V - I < 0.7$
Red supergiants	$16 < V < 21.5$	$1.0 < V - I < 2.5$
Red giants (SE)	$22 < V < 24$	$1.0 < V - I < 2.0$
Extreme AGB	$19.5 < I < 21$	$2.5 < V - I < 4.5$

3. Distributions of the Stellar Populations

The red giants are distributed smoothly in the disk. The most interesting feature in their distribution is the sharpness of the disk edge as illustrated by Fig. 2. The transition between the disk and the halo occurs within about $3.5'$ or 900 pc at the assumed distance of 925 kpc (from Cepheids: Feast, this symposium), the disk radius being about 11 kpc. This implies that the stellar orbits must have very low eccentricities at the edge of the disk.

The distribution of the extreme AGB stars (not displayed) is also very smooth showing that they are old enough to have lost the memory of the arms where most of them were probably born.

Conversely, the blue stars are distributed very irregularly. They trace a two-arm spiral structure and many, but not all, are gathered in associations. This is illustrated in Figs. 3, 4 and 5.

Finally, the distribution of the red supergiants (not displayed) also shows the spiral structure, although less contrasted. The difference with the blue stars comes in part from contamination with Galactic red stars which are distributed uniformly (Galactic contamination is negligible for the blue stars), and in part from the fact that the red supergiants are older and have had time to partly move away from the spiral arms.

4. Young Blue Stars and Gas

We now compare the distributions of the blue stars as defined in Table 1 with those of atomic and molecular hydrogen. HI maps of M33 have been published

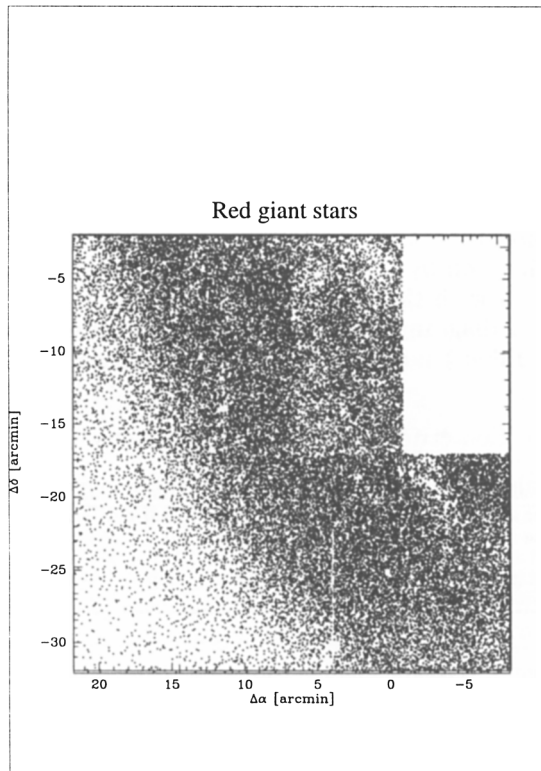


Figure 2. The distribution of the red giants in the SE part of M33. Mark the sharp edge of the disk. The total number of objects displayed on this field is about 40 000. Notice that on the upper central right CCD the completeness limit degrades, hence this area contains fewer objects. This CCD should not be considered here. Small empty areas are due to foreground bright stars obliterating their direct neighborhood on the CCD image.

by many authors. The most interesting for our purpose are the interferometric maps of Newton (1980) and of Deul & van der Hulst (1987). The latter map results from the Westerbork Synthesis Radio Telescope with the addition of short-baseline information from Effelsberg 100-m observations. Corbelli et al. (1989) have done low-resolution but extremely sensitive HI observations with the Arecibo telescope, which show that atomic hydrogen extends over 2° , very far from the limits of the two previous observations. A field including the nucleus of M33 has been mapped in the CO(1–0) line at 2.6 mm with the Amherst radiotelescope (Loinard et al., in preparation), using the same set-up as described by Loinard et al. (1996).

Figures 3 and 4 show the superimposition of HI line contours and CO line contours respectively, over the map of blue stars for a field in the central region of M33. One can see that while the gas and the blue stars are all roughly tracing the

spiral structure, the detailed correspondance between the three tracers is loose. This can only be due in part to extinction. There are blue stars in regions with little gas, and gas concentrations with or without associated blue stars. The South arm which is conspicuous on the figures is of particular interest in this comparison. This arm has been considered by Courtès & Dubout-Crillon (1971) and by Dubout-Crillon (1977) as the archetype for galactic shock-wave triggered star formation. If this is the case one should find a clear segregation between gas and stars of different ages through the arm. Such a segregation is not obvious in Figs. 3 and 4, and the red supergiants are also located like the blue stars, in spite of being older in the average. In general, the evidence for galactic shock-triggered star formation is becoming increasingly meager. Conversely, there is increasing evidence in favor of supercloud formation and subsequent star formation by gravitational collapse of gas gathered in density waves or other disk instabilities (Elmegreen 1994).

The comparison between the distributions of H I and of blue stars on the edge of the disk is also of interest. Fig. 5 shows the superimposition of H I contours from Deul & van der Hulst (1987) with blue stars in the SE region of M33. It is clear that, in spite of the presence of H I at larger radii, star formation stops when the column density of H I is smaller than $\simeq 3 \cdot 10^{20}$ atom cm^{-2} , corresponding to the first contour. A comparison with the maps of Newton (1980) and of Corbelli et al. (1989) gives similar results. Note that the 200 nm UV emission mapped by Buat et al. (1994) also disappears at this column density. In M31, star formation ceases at an H I column density of $\simeq 6\text{-}8 \cdot 10^{20}$ atom cm^{-2} which after deprojection corresponds to the same face-on column density as for M33. What is the meaning of this threshold? At least two explanations are possible:

- Stars form only when there is molecular hydrogen, and the threshold for star formation corresponds to the threshold for H₂ formation. The threshold for abundant formation of H₂ is at a column density of about $3 \cdot 10^{20}$ atom cm^{-2} in the solar neighbourhood (Savage et al. 1977; Reach et al. 1994; Boulanger et al. 1996). However, this might just be a coincidence, the threshold for H₂ formation being sensitive to the ultraviolet radiation field and to other parameters (see eqn. 3 of Reach et al. 1994).
- There is a threshold for instability in the gas and subsequent star formation. Kennicutt (1989) has proposed a simple criterion for gravitational instability but acknowledges that it fails for M33. Elmegreen (1995) has proposed another criterion for the two-fluid instability in the star + gas system: he defines an instability parameter Q_{eff} which depends on the surface density and velocity dispersion of both the stars and the gas. Further studies are required to see if this criterion works for both M31 and M33.

More generally, our data should allow to reconsider the law of star formation in galactic disks as pioneered by Madore et al. (1974) for M33.

5. The Halo of M33

Figure 6 presents the V , $V - I$ color-magnitude diagram for stars in the halo of M33. The giant branch is well defined and the horizontal branch is marginally

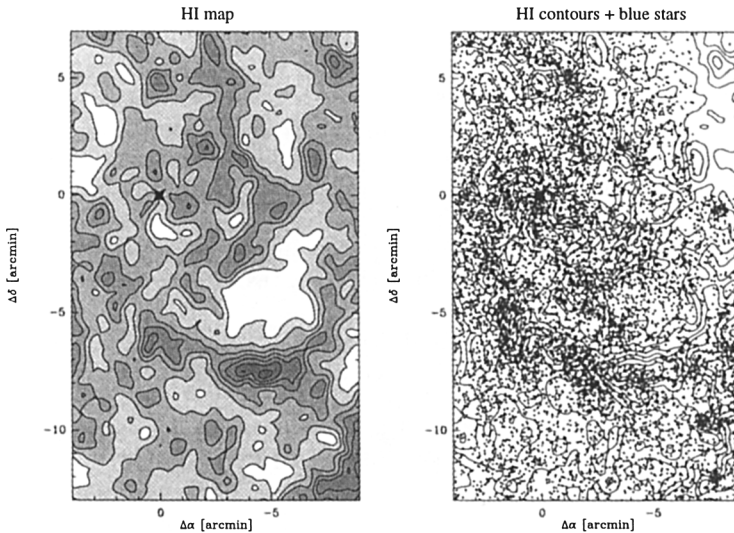


Figure 3. Comparison between the distribution of young blue stars and of H I in a region of the central disk of M33. For clarity, the H I map alone is shown on the left panel and the superimposition of the stars and of H I (contours) on the right panel. Coordinates are offsets with respect to the nucleus (diamond) at $\alpha(\text{J2000})=1\text{h }33\text{m }50.9\text{s}$, $\delta(\text{J2000})=30^\circ 39' 37''$. The H I contours correspond to column densities of 3 to 21 by steps of 3 in units of 10^{20} atom cm^{-2} . The FWHM resolution of the H I map is $12'' \times 24''$ ($\alpha \times \delta$). The H I map is from Deul & van der Hulst (1987).

seen at $V \simeq 25.5$, near the completeness limit. In order to compare this HR diagram with that of globular clusters, we need to know the reddening. The average between the determinations from the 21-cm line (e.g. Hartmann 1994) and from the foreground stars (Johnson & Joner 1987) is $E(B - V) = 0.06$ mag with an uncertainty of about 0.02 mag. This corresponds to $A_V=0.19$ mag, $A_I=0.11$ mag and $E(V - I) = 0.08$ mag with the same extinction law as used by Fusi Pecci et al. (1996). Comparing our $I, V - I$ color-magnitude diagram with the dereddened diagrams of template globular clusters given by Da Costa & Armandroff (1990) we arrive at the following conclusions:

- With the assumed distance modulus $(m-M)_0 = 24.82$, corresponding to a distance of 925 kpc and the reddening given above, the mean metallicity of the halo is $[\text{Fe}/\text{H}] = -1.0$ and there is a metallicity spread from $\simeq -0.6$

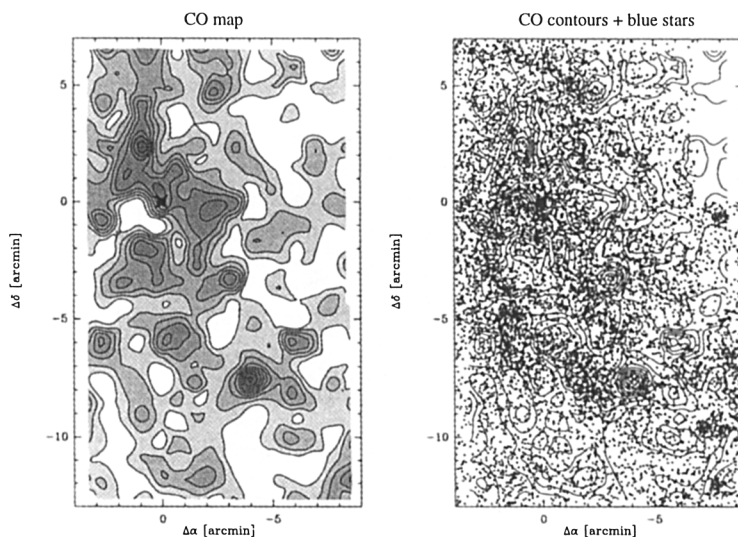


Figure 4. Comparison between the distribution of young blue stars and of CO(1-0) in a region of the central disk of M33. Presentation and coordinates as for Fig. 3. The CO contours corresponds to integrated line intensities of 0.5 to 4.5 K km s^{-1} by steps of 0.5 K km s^{-1} . The FWHM resolution of the CO map is $45''$. The CO map is from Loinard et al., in preparation.

to $\simeq -1.5$. These determinations are not very sensitive to the reddening because of its small value (possible changes by at most ± 0.1 dex).

- However, the derived metallicity is sensitive to the adopted distance. One can vary the distance modulus by ± 0.2 mag (± 80 kpc) without damaging too much the compatibility of the colour-magnitude diagram with the template diagrams. The shape of the red giant branch thus confirms the adopted distance modulus within ± 0.2 mag. The mean $[\text{Fe}/\text{H}]$ would change from -0.8 to -1.2 from the near to the far distance.

Due to the much better statistics and template clusters, our value of the metallicity of the halo of M33 supersedes the value of -2.2 given in the pioneering paper of Mould & Kristian (1986). For M31, we derive from our observations $[\text{Fe}/\text{H}] \simeq -0.6$, the same value as given by them.

Acknowledgements. We thank Eric Deul and Thijs van der Hulst for communicating the H I and CO maps of M33. We thank the Terapix data center for the use of its facility to reduce and analyse the data.

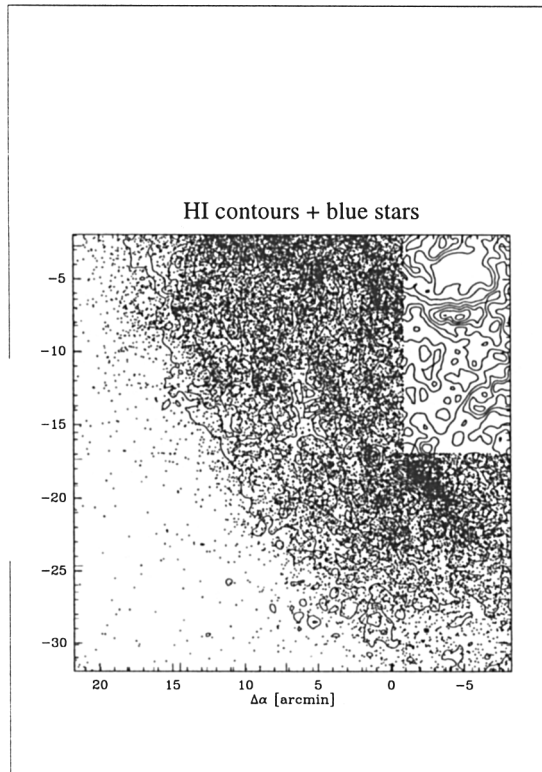


Figure 5. Comparison between the distribution of young blue stars and of HI in the SE region of M33. Coordinates are offsets with respect to the nucleus. The HI contours correspond to column densities of 3 to 21 by steps of 3 in units of 10^{20} atom cm^{-2} . The FWHM resolution of the HI map is $12'' \times 24''$ ($\alpha \times \delta$). The map is from Deul & van der Hulst (1987).

References

- Bertin, E., Arnouts, S. 1996, *A&AS*, 117, 393
 Boulanger, F., Abergel, A., Bernard, J.-P., Burton, W.B., Désert, F.-X., Hartmann, D., Lagache, G., Puget, J.-L. 1996, *A&A*, 312, 256
 Buat, V., Vuillemin, A., Burgarella, D., Milliard, B., Donas, J. 1994, *A&A*, 281, 666
 Corbelli, E., Schneider, S.E., Salpeter, E.E. 1989, *AJ*, 97, 390
 Courtès, G., Dubout-Crillon, R. 1971, *A&A*, 11, 468
 Cuillandre, J.-C., Lequeux, J., Mellier, Y., Allen, R.J. 1999, *A&A*, in preparation
 Da Costa, G.S., Armandroff, T.E. 1990, *AJ*, 100, 162
 Deul, E.R., van der Hulst, J.M. 1987, *A&AS*, 67, 509
 Dubout-Crillon, R. 1977, *A&A*, 56, 293

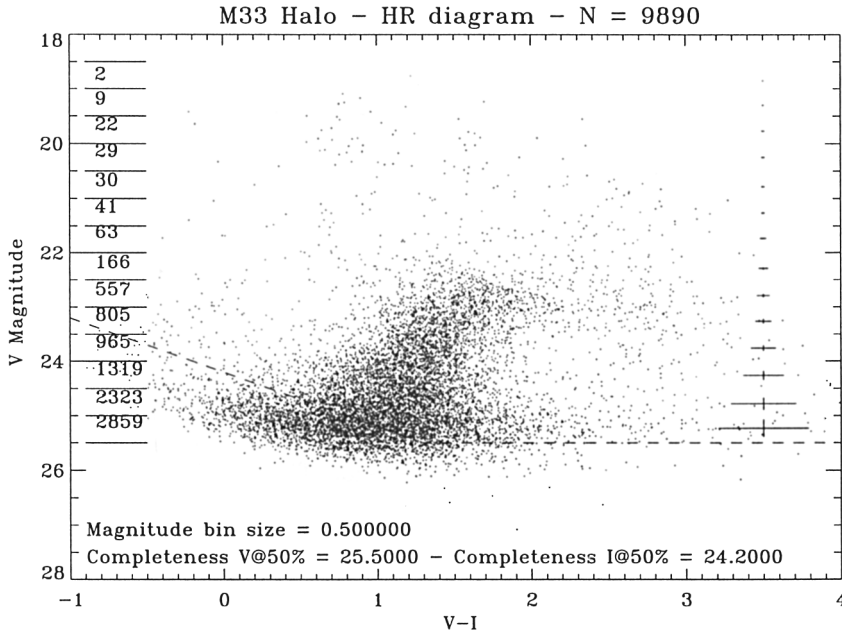


Figure 6. The V , $V - I$ color-magnitude diagram for stars in a field in the halo of M33. The dashed line is the estimated 50% completeness limit. Estimated $1-\sigma$ errors in $V - I$ are indicated on the right.

Elmegreen, B.G. 1994, ApJ, 433, 39

Elmegreen, B.G. 1995, MNRAS, 275, 944

Fusi Pecci, F., Buonanno, R., Cacciari, C., Corsi, C.E., Djorgovski, S.G., Federici, L., Ferraro, F.R., Parmeggiani, G., Rich, R.M. 1996, AJ, 112, 1461

Hartmann, D. 1994, PhD thesis, Leiden Observatory

Johnson, S.B., Joner, M.D. 1987, AJ, 94, 324

Kennicutt, R.C. 1989, ApJ, 344, 685

Landolt, A.U. 1992, AJ, 104, 340

Lequeux, J., Guélin, M. 1996, in: *New Extragalactic Perspectives in the New South Africa*, (eds.) D.L. Block & J.M. Greenberg, Dordrecht: Kluwer, p. 422

Loinard, L., Dame, T.M., Koper, E., Lequeux, J., Thaddeus, P., Young, J.S. 1996, ApJ, 469, L101

Madore, B.F., van den Bergh, S., Rogstad, D.H. 1974, ApJ, 191, 317

Mould, J., Kristian, J. 1986, ApJ, 305, 591

Newton, K. 1980, MNRAS, 190, 689

Reach, W.T., Koo, B.-C., Heiles, C. 1994, ApJ, 429, 672

Savage, B.D., Drake, J.F., Budich, W., Bohlin, R.C. 1977, ApJ, 216, 291

Discussion

Pritchett: (1) Can you rule out the possibility that your M33 halo field is in actual fact an old disk field, in which star formation stopped > 10 Gyr ago? (2) If not, could you compare the radial distance of your field from the centre of M33 with the radial distance of the Mould & Kristian (1986) field? [i.e. is it possible that the MK86 field is further out and really is a halo field, (and that the halo has $\text{Fe}/\text{H} = -2$)]

van den Bergh: What is the reason for the systematic difference between the M31 and M33 halo $[\text{Fe}/\text{H}]$ values of Lequeux and of Mould & Kristian?

Lequeux: I agree that the halo field we studied is so near to the edge of the disk that it might correspond to an old disk. Unfortunately the situation is not as favourable as for M31, a very inclined galaxy for which studies along the minor axis are possible and clearly concern the halo. The Mould & Kristian field is within our image. The $[\text{Fe}/\text{H}]$ difference is due to our better star statistics, hence a better-defined giant branch, and also to a better globular cluster metallicity calibration since 1986. Note that recent independent determinations of the halo metallicity of M31 and M33 agree with ours.

Freeman: Your CMD for the halo of M33 seemed to show a broadened giant branch; could you comment on the abundance spread?

Lequeux: Indeed the width of the RGB looks broadened, although less than for the halo of M31. We have not yet analysed the corresponding metallicity spread accurately.